https://doi.org/10.5194/wes-2025-110
Preprint. Discussion started: 25 August 2025

eawe european academy of wind energy
Open Access WIND ENERGY SCIENCE DISCUSSIONS

Hydro-elastic coupling effect on the dynamic global response of a spar-type floating offshore wind turbine

Cesar. Aguilera [1], Romain. Ribault [2], Jerome. De-Lauzon [3], and Adrien. Hirvoas [2]

[1]Sercel, 16 Rue du Bel air, 44470 Carquefou, France
[2]France energies Marines, 525 Av. Alexis de Rochon, 29280 Plouzané, France
[3]Bureau Veritas, 1 place Zaha Hadid, 92400 Courbevoie, France

Correspondence: Cesar. Aguilera (cesar.aguilera@sercel.com)

Abstract. Designing floating wind turbine systems requires integrated load assessments (ILA) using fully coupled hydro-servo-aero-elastic models. While potential flow models are commonly used to represent floater hydrodynamics for mooring system design and motion estimation, the floater is tipically assumed as rigid body. This assumption can significantly impact tower eigenfrequency calculations, particularly for large floaters. In this study, we investigate these effects using in-situ sensor data from the Zefyros 2.3MW spar wind turbine. We detail the methodology employed to accurately determine tower's eigenfrequencies. A rigid floater without added mass resulted in a 37% error compared to measured modes. Incorporating floater flexibility and added mass reduced this error to 5%, and further to 3% with blade flexibility. These discrepancies highlight the necessity of refining the hydro-servo-aero-elastic model to match the eigenfrequencies derived from finite element hydro-structural analyses. We present potential model adjustments and discuss their impacts. After implementing one model modification, we present the results and illustrate the updated model validation process.

1 Introduction

Offshore wind energy has grown rapidly over the past decade, with a threefold increase in capacity between 2012 and 2022. During this period, a significant average annual wind capacity of 55GW was added; and 75GW only in 2022 (IRENA , 2023). According to the 1.5°scenario (IRENA , 2023), wind energy will be one of the largest sources of electricity worldwide with a prediction of 10,300 GW by 2050.

At the same time, the development of wind energy faces the problem of having a high levelized cost of energy (LCOE) compared to other sectors. Given the collaborative research efforts during the design and development, government policies, and the significant increase in asset production in recent years, the domain has considerably reduced the LCOE of Floating Offshore Wind Turbines (FOWT) making them more cost-competitive (WindEurope , 2020).

One strategy for the cost reduction is to increase the individual asset power generation, which increases at the same time the general structural size. As the floater structure also increases in size, this leads to a design of more flexible support structures. The design of the support structure for FOWTs is not an easy task. This is mainly due to the complex phenomena that must be considered as these assets are deployed in very hostile environments (European Commission , 2019). Thus, the continuous evolution of the design of larger structures is now a concern in the design community.

https://doi.org/10.5194/wes-2025-110
Preprint. Discussion started: 25 August 2025

eawe european academy of wind energy
Open Access WIND ENERGY SCIENCE DISCUSSIONS

Currently, only a few FOWTs are operational. Zefyros (shown in figure 1), is one them. This wind turbine is located 11 km far from the coast of Norway and now owned by Unitech. It is the first multi-megawatt floating turbine in the world (Skaare et al. , 2014). The first numerical model of Zefyros was presented in the work of Skaare et al. (2007). In this work, the structure was modeled using a coupled simulation based on two different software's, SIMO/RIFLEX and HywindSim, developed by Marintek and Risø National Laboratory respectively. Both simulators solve their own dynamic equilibrium equations in time domain. A scaled set of tests cases were carried out by Ocean Basin Laboratory at Marintek with the objective to compare the results of an integrated coupled simulation tool outputs with experimental data. A good agreement was shown between simulation and measurement data.

Many studies using aero-hydro-servo-elastic simulations of FOWTs (e.g., (C.P.M. Curfs , 2015; Cheng et al. , 2015; Zhang et al. , 2020)) consider tower and blade flexibility. However, when focusing on mooring design or FOWT motion, potential flow models are often used for floater hydrodynamics. Although these models accurately capture hydrodynamic loading, they typically assume a rigid floater. This rigidity not only precludes calculating internal floater loads but also impacts tower eigenfrequency calculations, potentially affecting tower dynamic response.

The effect of the floater flexibility on the global dynamic responses of a 15MW semi-submersible floating wind turbine has been highlighted in the work of Haoran Li et al. (2023). Zhixin Zhao et al. (2022) have proposed a method to include flexibility of large-volume substructures based on an iterative procedure between radiation-diffraction solver WAMIT and HAWC2 software's for a spar-type substructure. In this work, a dynamic comparison of the global response between rigid and flexible model was performed, showing that flexibility provides additional information to derive more accurate sectional loads.

As it has been shown, this flexibility effect is addressed in the literature for different floating support structure types and wind turbine sizes. In DNV-RP-0286 (DNV-GL , 2019) it is mentioned that this hypothesis may be sufficient in certain cases, and before implementation, it should be demonstrated that the flexibility of the floating device does not have a significant influence on the response of the turbine. NR572 (Bureau Veritas , 2015) also mention that hydro-elasticity needs to be considered where appropriate. However, today there is no clear guidance on the recommended practices for the validity and application of the substructure rigid body simplification during the design phase.

This article details a methodology to accurately calculate tower eigen-frequencies at design stage and integrate floater flexibility effect into the aero-hydro-servo-elastic simulations. We demonstrate the impacts of floater rigid body assumption on tower eigenfrequency calculation, using in-situ sensor data from the Zefyros 2.3MW spar wind turbine. Section 1.1 briefly introduces the Zefyros wind turbine. In Section 2.1, we describe the measurement campaign and the estimation of tower eigenfrequencies, among other dynamic parameters, using the S-Morpho measurement system. In Section 2.2, we describe the numerical models. The subsection 2.2.1 provides some theoretical background on the hydro-structural model used for modal analysis and reference calculation of the tower eigenfrequencies. Then, in Section 2.2.2, we describe the initial aero-hydro-servo-elastic simulation model implemented in OpenFAST. In Section 2.2.3, is presented the potential simulation model adjustments, discussing their limitations and impacts. For the tower's eigenfrequency calculation from time-domain simulation

https://doi.org/10.5194/wes-2025-110
Preprint. Discussion started: 25 August 2025

Figure 1. Zefyros, the world's first multi-megawatt FOWT UNITECH (2022). Credits: Unitech Energy Group

results, we used an Operational Modal Analysis (OMA) tool described in Section 2.2.4. In section 2.3 we describe the load cases we used to run the aero-hydro-servo-elastic models in order to assess tower eigenfrequency in time domain simulation and identify a potential modification of the global dynamic tower response . Section 3 is dedicated to the discussion and the presentation of the results.

1.1 Description of Zefyros floating wind turbine

Unitech Zefyros is a floating spar offshore wind turbine originally installed as Hywind Demo by Equinor (Statoil) at approximately 11 kilometres of the west cost of Karmøy (Norway). The floater is based on a cylinder shape submerged vertically and connected to a steel tower. Having a spar-type substructure, the structure is stabilized due to the long distance between the center of gravity and center of buoyancy. This system is supporting a Siemens 2.3-MW wind turbine with a rotor diameter of 82.4 meters.

https://doi.org/10.5194/wes-2025-110
Preprint. Discussion started: 25 August 2025

eawe european academy of wind energy
Open Access WIND ENERGY SCIENCE DISCUSSIONS

The system is fixed to the seabed by three mooring lines consisting of hybrids wires and clump weights. The length of each line is approximately 800 metres.The hull is ballasted with gravel and water. The main particulars of Zefyros are given in Table 1. For a detailed description of the structure refer to the work of Sjur Neuenkirchen Godø (2013).

Table 1. Wind turbine characteristics.

Parameter	Value/Unit
Turbine power	2.3 MW
Turbine weight	138 tons
Draft hull	100 m
Nacelle height	65 m
Rotor diameter	82.4 m
Water depth	220 m
Mooring	3 lines
Diameter at water line	6 m
Diam. submerged body	8,3 m
Rotor speed	6 – 18 rpm
Wind speed range	3 – 25 m/s

2 Methodology

2.1 Measurements performed on 2.3MW Zefyros wind turbines

Dynamic and static measurement data was collected continuously during two years. This acquisition was done in the framework of DIONYSOS project using the S-Morpho system. Outputs of the sensor system include, three-axis accelerations, magnetic field, and temperature at a sampling frequency of $40Hz$. Six sensors were installed along the Zefyros tower in May 2022, approximately 30° west-north. The sensors were positioned at 17, 33, 41, 49, 57 and 63 meters above sea level. The local sensor reference frame was fixed to the tower reference frame, and the X and Y direction corresponds to the fore-aft and side-to-side movement respectively, and the Z as vertical movements. On figure 2 are shown the first two sensors installed on the tower. As the tower is made of steel, all sensors were fixed by two powerful magnets per unit. A general view of the positioning is depicted on figure 4. For more details about the sensor system please refer to (Redoute, T. , 2020).

https://doi.org/10.5194/wes-2025-110
Preprint. Discussion started: 25 August 2025

Figure 2. Sensor position along the tower.

2.1.1 Modal Identification of Zefyros Tower From Measurements

The simulation of the dynamic behavior of a wind turbine is strongly dependent on the accuracy of the numerical model. Therefore, calibration of the model is required based on reliable experimental data to correctly reproduce the dynamic response of the asset. The experimental selected data for this calibration were the global modal parameters.

The Zefyros wind turbine is equipped with a yaw system that allows the rotation of the nacelle to keep it facing the wind direction. This property makes the modal analysis more complex for wind turbines, as the modal deformation of the structure is dependent on the nacelle orientation (Gustavo Oliveira et al. , 2018). To overcome the problem of the nacelle moving reference frame and the tower fixed reference frame, the following coordinate transformation was performed using the nacelle orientation angle from the SCADA data, provided by Unitech Energy Group :

$$\begin{bmatrix} x'(t,\theta) \\ y'(t,\theta) \\ z'(t,\theta) \end{bmatrix} = R(\theta) \cdot \begin{bmatrix} x(\theta) \\ y(\theta) \\ z(\theta) \end{bmatrix} \tag{1}$$

Where the variables x and y contain the raw acceleration data, variables x' and y' are the new transformed accelerations and corresponds to the yaw angle θ of a 10 min averaged. $R(\theta)$ is the three axes matrix rotation. The mentioned coordinate transformation made possible to represent the acceleration signal of the sensors and project them into the fore-aft and side-to-side directions of the turbine, horizontal orthogonal to the rotor plane and horizontal parallel direction to the rotor plane respectively. After preprocessing, the transformed acceleration data is processed in a continuous manner using OMA techniques for wind turbine structures when external excitation cannot be measured (van Vondelen, A. et al. , 2022). As example, in figure 3 is shown the modal tracking of the second fore-aft and side-to-side tower modes during December 2022 as the pink and red

https://doi.org/10.5194/wes-2025-110
Preprint. Discussion started: 25 August 2025

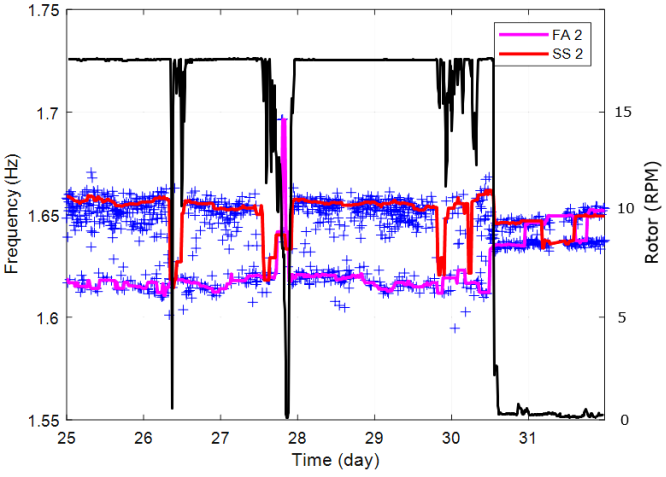

Figure 3. Plot of the second tower natural frequency tracking correlated with the rotor rotation during December 2022

lines respectively. The black line depicts the time series of the rotor rotation in RPM from SCADA data. This image shows the effect that has the rotor rotation on the tower modal frequencies.

The modal analysis algorithm used for the study is the so-called covariance-driven stochastic subspace identification (SSI-COV) method with 6 reference channels and for 20 minutes time windows. For more detail of the method, please refer to (Masjedian, M.H. and Keshmiri, Mehdi , 2009). The emerged frequencies of the structure are shown in table 4. A more detailed description about the calculation methodology can be found in the document of SERCEL (2024).

2.2 Numerical models

In the following subsections the methodology calculation on each software is briefly described. It must be mentioned that Homer has been used as the offshore modal analysis tool, solving the classic equation of motion (equation 3). Regarding the coupled dynamic time-domain simulations for wind turbines, an OpenFAST model was tested. A summary of the two numerical model characteristics is given in table 2. A more detailed description is given in the following sections.

Table 2. Model main characteristics in function of the numerical software.

software	Flexible floater	Rigid nacelle	Flexible blades
Homer	✓	✓	x/✓
OpenFAST	x	✓	✓

https://doi.org/10.5194/wes-2025-110
Preprint. Discussion started: 25 August 2025

eawe european academy of wind energy
Open Access WIND ENERGY SCIENCE DISCUSSIONS

2.2.1 Hydro-Structure Model To Perform Tower's Eigenfrequency Reference Calculation

To calculate the reference eigenfrequencies of the tower, the analysis was carried-out in Homer, an Hydro-structure software with modal analysis capability developed by Bureau Veritas (Malenica, Š et al. , 2013). The model implemented in Homer describes the full mechanical FOWT system and is derived from an ANSYS model (figure 4). The floater and tower are discretized with beams or shell elements. Rotor Nacelle Assembly and mooring system stiffness are modeled. Blades are also modeled as flexible elements.

The hydro-elastic analysis performed in Homer relies on the decomposition of the structural response of the floating wind turbine on its N first dry vibration modes. Instead of solving a 6-by-6 linear problem, the dimension of all matrices (mass, added mass, stiffness) is increased to $6+N$.

The first step in the coupled analysis is therefore a dry modal analysis of the structure. When the flexible modes have been chosen, the hydrostatic stiffness is computed for the N vibration modes, as well as for the six rigid body motions (surge, sway, heave, roll, pitch, and yaw). The hydrodynamic radiation boundary value problem is then solved by Hydrostar for the $6+N$ modes, and the added mass matrix is then assembled. Finally, the wet eigen-modes and frequencies are computed. The method is rather well known and has been the subject of many scientific publications (Malenica, Š et al. , 2008). The pre-stressing at hydrostatic equilibrium is not considered in this analysis; its influence is assumed to be small.

Bureau Veritas Hydrostar software is used to solve the radiation boundary value problems for the rigid body motions, as well as for the vibration modes. For each vibration mode, the additional body boundary condition becomes:

$$\frac{\partial \varphi_{Rj}}{\partial n} = \mathbf{h^j} \cdot \mathbf{n} \tag{2}$$

Where φ_{Rj} is the radiated velocity potential for mode j and $\mathbf{h^j}$ is the shape of mode j, interpolated from the finite element model to the hydrodynamic mesh. Once all radiation boundary value problems (6 rigid motions and N elastic modes) have been solved, the radiation pressures are computed at the center of the finite elements, and integrated to compute the added masses. The motion equation can then be written as (after removing the excitation forces and radiation damping):

$$(-\omega^2[M + A(\omega)] + [K + C])\{\xi\} = 0 \tag{3}$$

With $[K]$ the structural stiffness, $[C]$ the hydrostatic stiffness, $[M]$ the structural mass, $[A(\omega)]$ the added mass and $\{\xi\}$ the vector of modal amplitudes. For each frequency ω, the inverse of the total mass (including added mass) is computed and multiplied by the total stiffness. The resulting matrix is finally diagonalized for each frequency to find the wet eigen-frequencies and eigen-vectors. For each eigen-mode computed by the diagonalisation, the vibration frequency is obtained when the eigen-frequency matches the frequency used for the added mass.

$$[M + A(\omega)]^{-1}[K + C]\{\xi\} = \omega^2\{\xi\} \tag{4}$$

https://doi.org/10.5194/wes-2025-110
Preprint. Discussion started: 25 August 2025

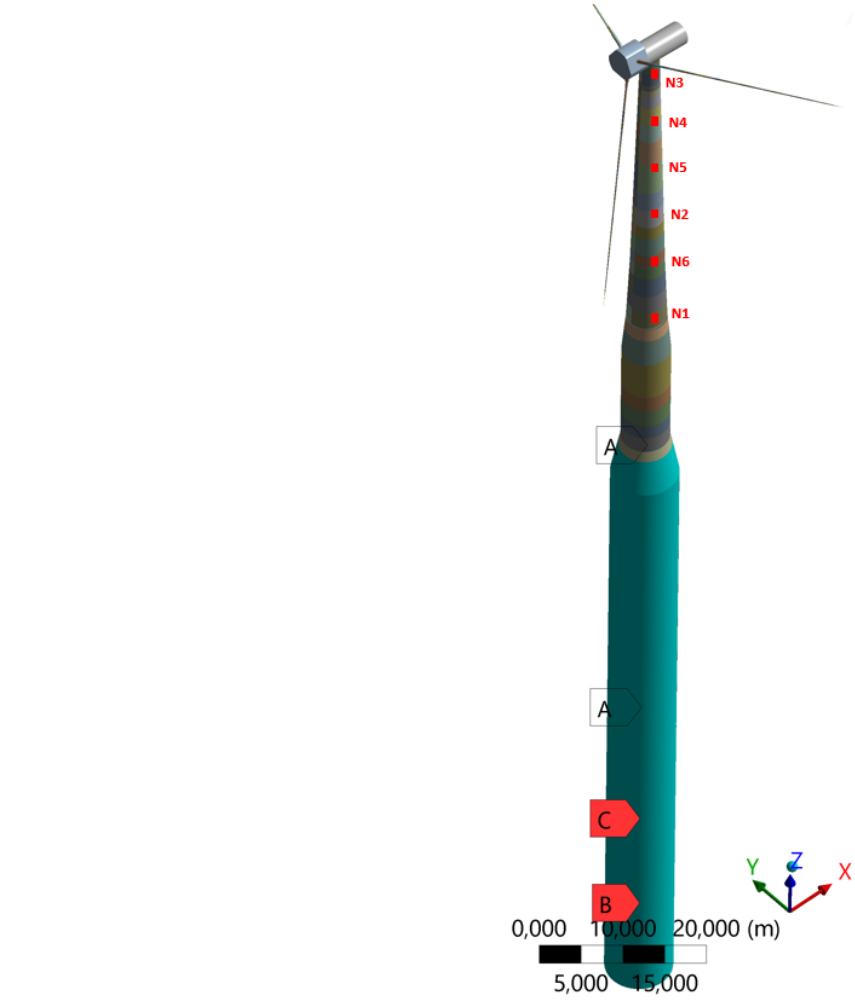

Figure 4. Graphic representation of the Homer shell element model

2.2.2 Initial Aero-Hydro-Servo-Elastic Simulation Model

OpenFAST (FAST stands for Fatigue, Aerodynamics, Structures, and Turbulence) is an open-source engineering code distributed by the National Wind Technology Center (NWTC) (Jonkman, Jason Mark et al. , 2005). This code is a nonlinear time-domain simulator that employs a combined modal and multibody structural-dynamics formulation. In our research, the numerical representation of the Zefyros system has been implemented within OpenFAST. This model assumes a rigid platform but accounts for the tower's flexibility, see Figure 5. The structural, hydrodynamic, and aerodynamic properties of the FOWT were configured based on publicly available documents and generic wind turbine data interpolation. The key properties defined include inertial characteristics of the nacelle, lift and drag profiles of the airfoil, along with mass and structural-elastic

https://doi.org/10.5194/wes-2025-110
Preprint. Discussion started: 25 August 2025

properties at various blade locations, inertial and structural-elastic characteristics of the drive train, mass and structural-elastic properties at specific tower locations, from the waterline to the tower's top, and inertial properties of the rigid spar.

To prevent drifting, the Zefyros platform is anchored to the seabed using three separate catenary mooring lines attached to anchors at the seafloor. For the numerical representation of mooring line dynamics, we used MoorDyn, a dynamic lumped mass model within OpenFAST (Hall, Matthew , 2015). This numerical modeling methodology leverages this model's capability to represent multi-segmented mooring lines, comprising diverse elements such as chains, unsheathed spiral ropes, and additional clump weights, as outlined in Hirvoas, A. (2022). The latest version of MoorDyn enables modeling two-leg bridles, significantly improving the yaw natural period from previous versions (Hall, Matthew , 2020).

Incorporating hydrodynamics into the numerical simulation requires accurately defining incident wave characteristics and hydrodynamic loading representations (Molin, Bernard , 2023). Within this OpenFast framework, HydroDyn is the module designed to calculate these hydrodynamic loads in the time domain (Jonkman, Jason et al. , 2014). To obtain the hydrodynamic loads acting on the rigid body platform, a pre-computation step using radiation-diffraction software with a second-order loading module is necessary to solve different hydrodynamic theories. Finally, in our full-scale study, we calibrated the mooring radius and the platform's displaced volume to match the system's natural periods with low relative errors, as evaluated using in-situ data.

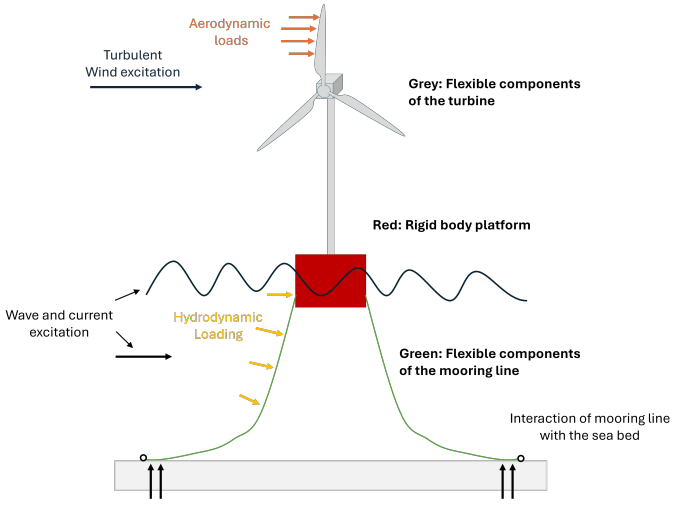

Figure 5. Schematic overview of the FOWT modeling approach in OpenFAST.

Additionally, we adapted the ROSCO NREL controller, as described in (Abbas, Nikhar J et al. , 2022), to the simulation model and conducted different dynamic load cases, comparing them with field measurements. The results show that the floating platform movements closely match the measured data, indicating good agreement as shown in Hirvoas, A. (2022).

https://doi.org/10.5194/wes-2025-110
Preprint. Discussion started: 25 August 2025

eawe european academy of wind energy
Open Access WIND ENERGY SCIENCE DISCUSSIONS

2.2.3 Possible aero-hydro-servo-elastic model modification and impacts

When it is required to modify the model aero-hydro-servo-elastic to match the simulation model's tower eigen-frequencies with the measured / calculated one, several approaches can be used. The first option to investigate is to make the floater a flexible body, using a beam element discretisation and distribute the hydrodynamic loading calculations over each beam element. This will provide access to internal loads of the floater, at the chosen discretisation scale. Two types of hydrodynamic models can be used :

1. Distributed potential flow hydrodynamic model.
2. Distributed Morison elements.

Thomsen, Jonas Bjerg et al. (2021) and Kun Xu et al. (2019), used a full Morison approach for the hydrodynamic model and beam elements for mechanical model of the floater. Such approach can lead to satisfactory FOWT global model with floater flexible models. However, Morison hydrodynamics model has its own limitations (V. Leroy et al. , 2021) and coefficients are not available for all floater shapes which makes the approach not applicable for some floater designs (Guignier, Lucie et al. , 2016).

To model the floater hydrodynamics with potential theory while modeling the floater as a flexible body, several initiatives explored equivalent approaches. They combine multi-body or additional generalized modes capabilities of radiation diffraction software (Wamit, Hydrostar, Diodore, etc…) with beam element models of aero-hydro-servo-elastic software (such as Orcaflex, Deeplines or SIMA):

- The radiation diffraction software calculates several hydrodynamic database (HDB) on a floater discretisation equivalent to the mechanical model discretization.
- The floater is mechanically modeled as an assembly of beam elements in aero-hydro-servo-elastic software and for each beam element, the corresponding HDB is associated.

This type of approach was applied to the Ideol's floater, using Ansys Aqwa as the radiation diffraction software and Orcaflex as the aero-hydro-servo-elastic software (Guignier, Lucie et al. , 2016); They used a multibody approach for the radiation-diffraction calculations with Aqwa. They discretized the floater in several compartments and calculated HDs including the hydrodynamic interactions between compartments. However, they needed to artificially separate the compartments in Aqwa code to avoid divergence of the calculations.

A similar but different approach was applied to a spar platform, supporting the DTU 10 MW by Xiaoming Ran et al. (2023); and a three-column semi-submersible floaters by Chenyu Luan et al. (2017) and by Haoran Li et al. (2023). They all used Wamit as a Radiation-Diffraction software and an in-house code to integrate panel pressure per floater sub-structure to compute the added mass, damping and excitation forces with a discretization adapted to the mechanical model of the floater.
In the above cited approaches, hydrodynamic interactions between sub-structures are taken into account, but the hydrostatic/hydrodynamic loads are not influenced back by floater flexibility. Chenyu Luan et al. (2017) acknowledged that the influence

https://doi.org/10.5194/wes-2025-110
Preprint. Discussion started: 25 August 2025

eawe european academy of wind energy
Open Access WIND ENERGY SCIENCE DISCUSSIONS

of the inertia loads and hydro loads induced by the flexible modes of the hull shall be investigated in future. To account for deformable modes of a floater contribution into hydrodynamic loads, within a small deformation assumption, Borg, Michael et al. (2016) proposed an iterative procedure between aero-hydro-servo-elastic (HAWC2) and WAMIT. Additional generalized modes calculation option may also be used de Lauzon Jérome (2024) and are available in Homer software. Xiaoming Ran et al. (2023) performed an experimental validation such an hydro-structural coupled model, demonstrating that internal floater loading estimations where more accurate with a distributed potential flow hydrodynamic model rather than with a Morison hydrodynamic model.

When the above approaches cannot be implemented other options are available :

1. Prolongate the tower mechanical model with a virtual element inside the floater and calibrate the mechanical properties to match the tower eigenfrequencies.
2. Modify the global stiffness modal parameter in OpenFast, such an option is available inside the Elastodyn file

In our case, the only feasible option was to modify the global tower stiffness. Indeed our OpenFAST model did not include the Subdyn module which would allow the tower prolongation below the floater/tower interface. Because the eigenfrequency mismatch was quite significant in our case, adding a small element at the bottom of the tower was not a workable option. It shall be noted that Hydrodyn and Subdyn modules were recently updated with the capabilities to model flexible floaters.

2.2.4 Verification tool of simulated tower frequencies and shapes

To check the tower eigenfrequencies of aero-hydro-servo-elastic model against the hydro-structure calculation model, it is required to perform a modal analysis on the aero-hydro-servo-elastic model. The aero-hydro-servo-elastic model are used to run time domain simulations where most of the physics in the wind turbine modeling are nonlinear. A specific linearization of a specific state-space is required to perform eigenanalysis. Most of the softwares have such modal analysis module included. In our OpenFast model, two options were available :

- the use of the linearization functionality included in the OpenFAST open-source code
- running OMA techniques on the OpenFAST output acceleration data.

Even thought the OpenFAST funcionality has been widely used and verified for FOWTs as demonstrated in (Johnson, Nicholas et al. , 2019), in this study the validation of the natural frequencies and shapes was estimated via OMA already used when estimating the modal parameters of measured data, described in section 2.1.1.

2.3 Load cases for evaluation of dynamic tower response in time domain calculations

The first stage on the proposed methodology consisted determining the sensitivity of the tower modes to the floater rigidity. In the second stage, the aero-servo-hydro-elastic model is adapted to take into account the flexibility of the floater. To do that, two

https://doi.org/10.5194/wes-2025-110
Preprint. Discussion started: 25 August 2025

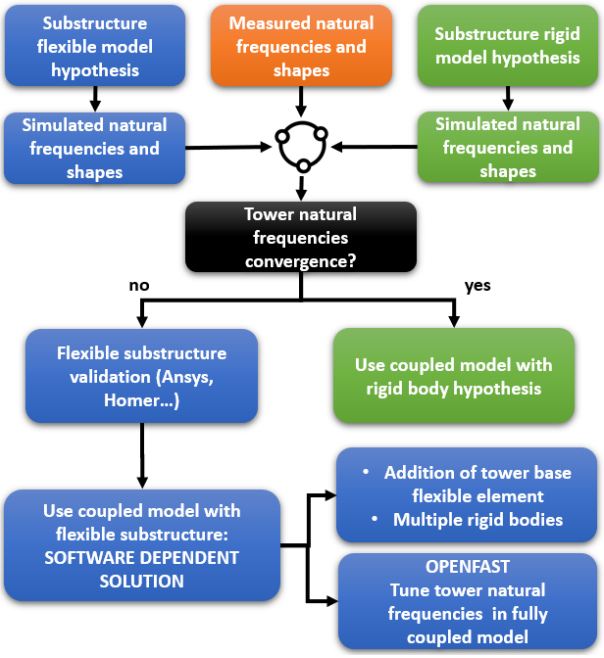

Figure 6. Schematization of the methodology followed in this study.

main load cases were analyzed to investigate the global response of the structure, in a low and rated condition. The criteria for low wind load condition was that wind should be lower than $12m/s$ with a significant wave height smaller than $2m$. For rated condition, the wind speed and wave height should have values around $13m/s$ and $3.5m$ respectively. In table 3 are described the set of input parameters of the two load cases. The time series of irregular wave elevation were modeled with a JONSWAP spectrum. The time-varying wind loads were calculated using Turbsim, a full-field turbulent-wind simulator (B. J. Jonkman , 2016).

Table 3. Load cases characteristics of 1 hour average values. Low condition of 02/12/2022 at 3 p.m. And Rated condition of 06/12/2022 at 10 p.m.

Load case	Low condition	Rated condition
Wave height [m]	1.36	3.3
Wave direction [°]	273	336
Wave period [s]	13	8
Wind speed [m/s]	1.92	15.1
Wind direction [°]	70.88	354.7

https://doi.org/10.5194/wes-2025-110
Preprint. Discussion started: 25 August 2025

eawe european academy of wind energy
Open Access WIND ENERGY SCIENCE DISCUSSIONS

3 Results and Discussion

This section is divided into two parts. Following the schema of figure 6 , this section shows the modal sensitivity analysis performed in Homer. In the second part, a spectral analysis of the measured acceleration and the simulation signals is presented.

A 1 hour simulation time was run for each load case in OpenFAST. To avoid the undesired model transient response, the first 300 seconds were eliminated, keeping the equivalent 1 hour simulation when the structure is in its stability position.

3.1 Sensitivity analysis

During this analysis, the effect on the tower modes of the following phenomena and component modeling was evaluated:

- the floater rigidity
- the hydrodynamic added mass
- the flexibility of the blades

This first sensitivity analysis was carried-out in Homer based on the shell model shown in figure 4. For the reference case, the rotor nacelle assembly (including the blades) and the floater were considered as rigid. To approximate the floater structure to the rigid hypothesis in the Homer model, the material Young modulus was increased from the steel value of $2.1E+11Pa$ to $1E+20Pa$.

On the upper graph in figure 7 is presented a diagram of the natural frequencies of the system. The first 6 modes correspond to the 6 degrees of freedom of a floating system. Very good agreement has been shown between measured and simulated values, indicating a good accuracy of the global mass and stiffness description of the system. A maximum error of 7% was estimated when comparing the yaw response. The average error of the 6 degrees of freedom is around 3%. Indeed, the rigid floater showed a minimum influence on the low frequency modes $(1^{st} - 6^{th})$.
On the contrary, the stiffness of the floater had great influence on the tower modes as is shown on the last four modes in the same image on figure 7. A higher error between measurements and simulated tower modes was encountered when considering the floater as rigid, with a higher value up to 33% for the second side-to-side tower mode. Conversely, when the floater is modeled as flexible, the four tower natural frequencies drops to better match the measured frequencies. A graphic representation of the first fore-aft coupled floater-tower mode shape is shown on the rigth image of figure 7

In the second analysis, the effect of the hydrodynamic mass was evaluated. When considering this extra mass , a decreas in the frequencies is exhibited, together with the average error down to 28% (column 4 in table 4). In the same token, the fifth column shows a more significant decrease of the tower frequencies when the flexibility of the floater is added on top of the additional hydrodynamic mass, with a drop in the average error down to 5%.
In the final analysis, the blades flexibility was considered,while the hub and nacelle were modeled rigidly. A rigid connection was imposed to join the blades root and the hub. The distributed blade structural properties were obtained from the SIMA

https://doi.org/10.5194/wes-2025-110
Preprint. Discussion started: 25 August 2025

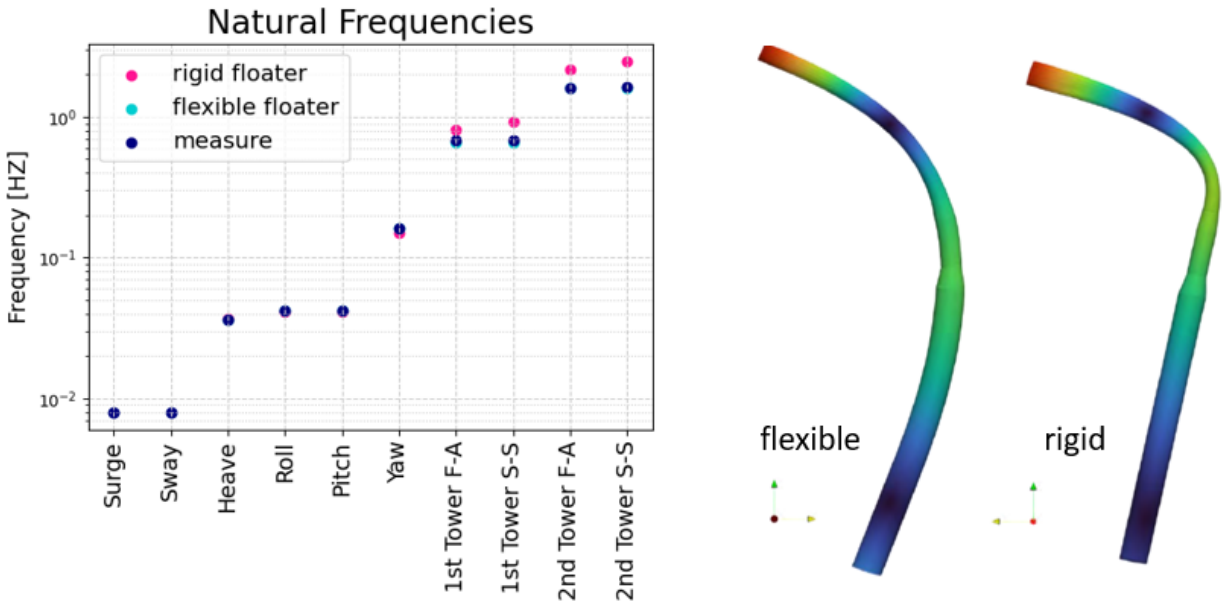

Figure 7. Plot of the measured and simulated natural frequencies of the system (upper figure). Graphical representation of the first fore-aft coupled floater-tower mode (lower image).

Table 4. Summary of the estimated tower natural frequencies from the sensitivity analysis.

	S-MORPHO	HOMER			
	Measure	Rigid/dry floater	Hydro added mass	Flexible floater	Flexible blades
1st tower SS	0.69	1.10	0.96	0.66	0.70
1st tower FA	0.69	1.14	0.98	0.66	0.72

model developed in (Homb, Hans Ranøyen , 2013).

The blade flexibility has an opposite effect in the tower modes. This flexibility has increased by a 7% the last results. It is important to note however, that this increase has diminished the error from 5% down to 3% as shown in the last column in table 4.

3.2 Spectral analysis

Thus far, it was verified that the rigid body floater modelling has important effects on the tower natural frequencies of the Zefyros FOWT. Therefore, this floater flexibility must be taken into account on the time domain simulation tool. To do this,

https://doi.org/10.5194/wes-2025-110
Preprint. Discussion started: 25 August 2025

eawe european academy of wind energy
Open Access WIND ENERGY SCIENCE DISCUSSIONS

the so-called tower adjustment factors were modify within OpenFAST simulator, inside the ElastoDyn file. These tower coefficients multiplies the global tower stiffness for the first and second tower mode in fore -aft and side-to-side directions. Only the two coefficients of the first tower mode were considered in this study.

In order to find the coefficient values, a manual trial and error tuning was done to fit the measured spectrum shown in figure 9. The individual coefficients values that fitted the measured frequencies were 0.397 and 0.400 for the fore-aft and side-to-side directions respectively.

To compare the time domain simulation outputs, 4 time domain simulations in OpenFAST were ran. The first two, for a low wind turbine condition with the original and the adjusted model. And 2 more for a rated condition. Hence, the graphs on figure 9 shows the acceleration spectrum comparison of the measured data (dark blue line), of the response of the rigid floater model (pink dashed line) and the tuned model (light blue dashed line) for low and rated conditions.

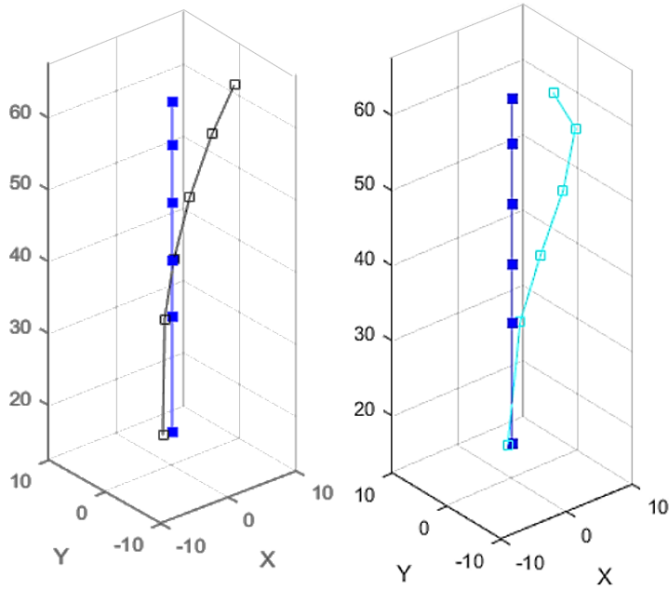

Figure 8. First and second tower mode shapes estimated from OpenFAST acceleration output data by OMA routine. Both images depicts the fore-aft direction..

The spectrum was calculated using a Welch's Power Spectral Density on python. The simulated dynamic response in the side-to-side direction (middle graph of figure 9) has shown a good agreement within the $0.05 - 3Hz$ frequency range. It is important to note how the tuned numerical model showed a sweep-off of the original frequency peak from $1.1Hz$ to $0.70Hz$ in the fore-aft and side-to-side spectrum that corresponds to first tower frequency. This was validated by applying OMA algorithm on the acceleration output data, as described in section 2.2.4. The result modal shape is illustrated on figure 8 that corresponds well to the first tower mode.

https://doi.org/10.5194/wes-2025-110
Preprint. Discussion started: 25 August 2025

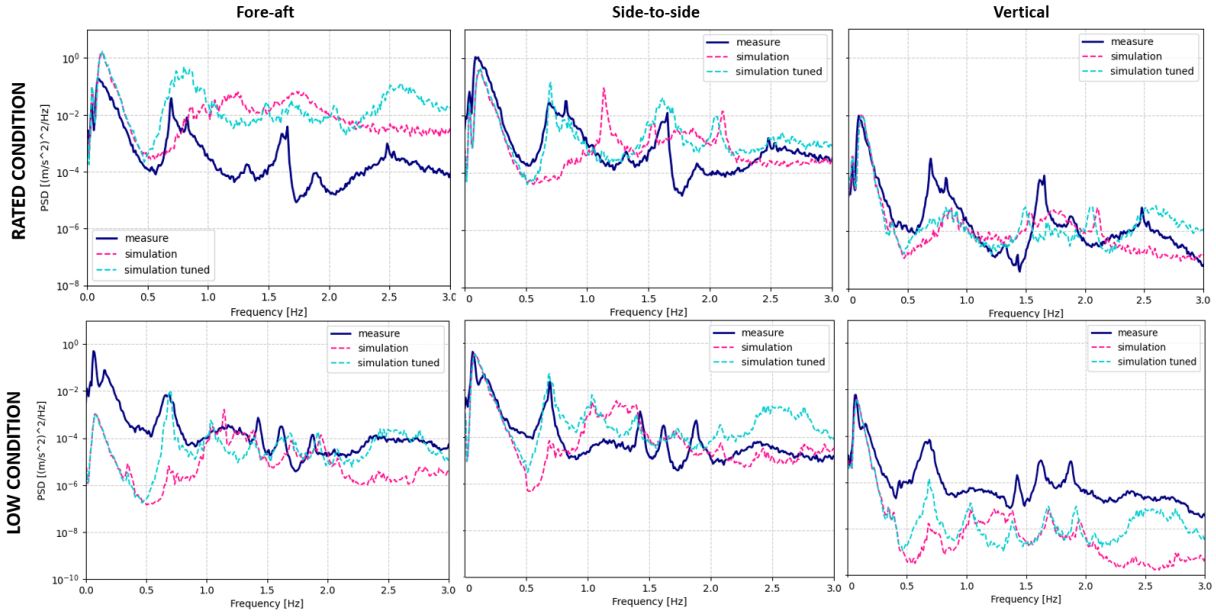

Figure 9. Spectrum of the measured and simulated acceleration of the sensor node 4 in function of the fore-aft, side-to-side and vertical directions. The dark blue line represent the measurement, the pink line is the response of the original model and the light blue line the response of the tuned model.

Taking into account the peak verification, it can be seen that the model fits very well the first tower mode at $0.69Hz$ and the harmonics due to the rotor rotation, the well known 3P and 6P at $0.83Hz$ and $1.66Hz$ respectively. The model showed lower accuracy in the low frequency content, i.e. between 0 and $0.05Hz$. This discrepancy may be due to the fact that second order hydrodynamic forces were not considered here.

In the fore-aft direction (left images in figure 9), the simulation response showed higher or lower amplitudes than the measured one along the whole analysed frequency range. The aforementioned may be due to several facts, as the uncertainty of the sensor position and direction, the uncertainty on the sensor localization inside the model in function of the tower discretization, etc.

As a result of the tuning process, and despite the dynamic response of the model got closer to the measure, the global tower stiffness has been modified, which had impacts on the system response. On top of that, the founded values are considerably low, which indicates a significant reduction on the tower rigidity. In the OpenFAST forum it is recommended to use this tower stiffness tuners for small adjustments, with values not smaller than 0.9. Usually, a stiffness modification in a system can be distinguishes on the low frequency content of a spectrum. Figure 10 shows the dynamic response before and after adjusting the tower stiffness. From the figure it can be seen that the adjustment has effects on low frequency content, for frequencies lower than $0.01Hz$. Similarly, the displacements and moments of the tower were analyzed to evaluate the influence of the coefficients modification. In the left image on figure 10 the displacements of the top of the tower are shown in the fore-aft and side-to-side

https://doi.org/10.5194/wes-2025-110
Preprint. Discussion started: 25 August 2025

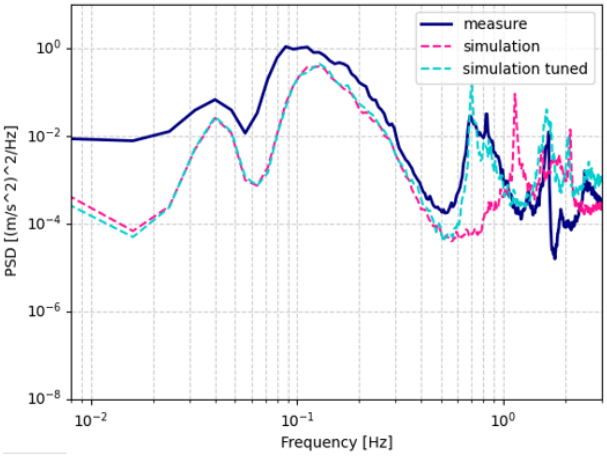

Figure 10. Power spectral density of the side-to-side dynamic response of sensor number 4. Rated condition.

directions. As expected, the amplitudes of the tower displacements increased as the tower stiffness decreased.
In contrast, the right image in the same figure shows that the tower-base bending moments on the frequency range of waves excitation $(0 - 0.5Hz)$ was not influenced by the global stiffness reduction of the tower.

4 Conclusion

This study investigates the effects the the floater rigid hypothesis, the hydrodynamic added mass and the flexibility of the blades have on the global dynamic response of the spar-type floating wind turbine Zefyros. A regular and still common practice in the wind turbine structural analysis is to consider the floater as a rigid body.
The tendency of the increasing energy production is directly related to the increase of the wind turbine size. As a result, when the structure increases, the rigid floater hypothesis loses validity. This has been corroborated during this study.It was demonstrated that the effect of the floater flexibility has great influence on the tower modes of a 2.3 MW spar-type, with a 37% error in comparison to the measured modes.

Hydro-servo-aero-elastic simulation tools can utilize a Morison hydrodynamic model to account for floater flexibility. When using flow potential hydrodynamic models of the floater, we observe that simulation tools are progressively integrating new functionalities to couple distributed hydrodynamic databases with mechanical beam element floater models.

When it is not possible to implement a flexible floater in the Hydro-servo-aero-elastic model due to software restrictions, it is generally feasible to modify the tower/floater boundary condition and calibrate the tower's eigen-frequency by adding a massless beam with a well-chosen length and stiffness below the tower. In OpenFAST, one possible solution is adjusting the global tower stiffness factors to properly fit the spectral response to the measured one. We do not recommend using this solution as it modifies the tower's mechanical model itself. However, we implemented it in our case due to limitations of the

https://doi.org/10.5194/wes-2025-110
Preprint. Discussion started: 25 August 2025

older OpenFAST version. We observed that this adjustment allowed us to match tower eigen-frequencies in the time domain simulations. It has shown to have minimal effects on the low-frequency content of the dynamic response, within the range of 0 to 0.01 Hz. Additionally, it increased the tower-top displacements as the tower becomes virtually less rigid. In contrast, the modification had a small influence on the tower-based bending moments.

Data availability. Data could be available on demand, in order with the contractual description of DIONYSOS project.

Author contributions. CA: Methodology, Software, Validation, Formal analysis, Investigations, Writing - original draft, Writing - review and editing, Visualization. RR: Methodology, Software, Investigations, Writing - original draft, Writing - review and editing, Project administration. JDL: Methodology, Software, Writing - Original Draft. AH: Methodology, Software,Writing - Original Draft

Competing interests. The authors declare that they have no conflict of interest.

https://doi.org/10.5194/wes-2025-110
Preprint. Discussion started: 25 August 2025

eawe european academy of wind energy
Open Access WIND ENERGY SCIENCE DISCUSSIONS

References

Homb, Hans Ranøyen.: Fatigue Analysis of Mooring Lines on the Floating Wind Turbine Hywind.2013.

WWEA: World Market for Wind Power Saw Another Record Year in 2021: 97,3 Gigawatt of New Capacity Added. 2019. https://wwindea.org/world-market-for-wind-power-saw-another-record-year-in-2021-973-gigawatt-of-newcapacity-added/

UNITECH: Dynamic cables for offshore wind farms. 2022. https://www.techtransfer.no/en/renewable-energy/unitech/

European Commission: Assessment of the final national energy and climate plan of France. 2023. https://commission.europa.eu/system/files/2023-12/SWD_Assessment_draft_updated_NECP_France_2023.pdf

European Commission : Summary of the Commission assessment of the draft National Energy and Climate Plan 2021-2030. 2019. https://energy.ec.europa.eu/system/files/2019-06/necp_factsheet_fr_final_0.pdf

Stadtmann, Florian and Rasheed, Adil and Kvamsdal, Trond and Johannessen, Kjetil André and San, Omer and Kölle, Konstanze and Tande, John Olav and Barstad, Idar and Benhamou, Alexis and Brathaug, Thomas and Christiansen, Tore and Firle, Anouk-Letizia and Fjeldly, Alexander and Frøyd, Lars and Gleim, Alexander and Høiberget, Alexander and Meissner, Catherine and Nygård, Guttorm and Olsen, Jørgen and Paulshus, Håvard and Rasmussen, Tore and Rishoff, Elling and Scibilia, Francesco and Skogås, John Olav: Digital Twins in Wind Energy: Emerging Technologies and Industry-Informed Future Directions. 2023.

Joyce Lee, Feng Zhao: Global wind repport 2021. 2021. https://gwec.net/wp-content/uploads/2021/03/GWEC-Global-Wind-Report-2021.pdf

Redoute, T.: Manuel d'utilisation du systéme neuron. 2020.

Global Wind Energy Council: GLOBAL OFFSHORE WIND REPORT 2023. 2023. https://gwec.net/wp-content/uploads/2023/08/GWEC-Global-Offshore-Wind-Report-2023.pdf

Hobbacher, AF and others: Recommendations for fatigue design of welded joints and components. 2016.

Skaare, Bjørn and Nielsen, Finn Gunnar and Hanson, Tor David and Yttervik, Rune and Havmøller, Ole and Rekdal, Arne: Analysis of measurements and simulations from the Hywind Demo floating wind turbine. 2015.

Goodfellow, Ian and Bengio, Yoshua and Courville, Aaron: Deep learning. 2016.

Ren21, K: Renewables 2021-Global Status Report: Tech. Rep.. 2021.

WindEurope: Wind Energy in Europe: 2021 Statistics and the Outlook for 2022-2026. 2021. https://windeurope.org/intelligence-platform/product/wind-energy-in-europe-2021-statistics-and-the-outlook-for-2022-2026/

Berahmand, Kamal and Daneshfar, Fatemeh and Salehi, Elaheh Sadat and Li, Yuefeng and Xu, Yue: Autoencoders and their applications in machine learning: a survey. 2024.

Susan Gourvenec: Floating wind farms: how to make them the future of green electricity. 2020.

Nava, V. and Ruiz-Minguela, P. and Perez-Moran, G. and Rodriguez Arias, R. and Lopez Mendia, J. and Villate-Martinez, J.-L.: Installation, Operation and Maintenance of Offshore Renewables. 2019.

Schlechtingen, Meik and Santos, Ilmar Ferreira and Achiche, Sofiane: Wind turbine condition monitoring based on SCADA data using normal behavior models. Part 1: System description. 2013.

Schlechtingen, Meik and Santos, Ilmar Ferreira: Wind turbine condition monitoring based on SCADA data using normal behavior models. Part 2: Application examples. 2014.

Aguilera C. and Desbazeille M.: 20240305 DIONYSOS WP04 Task4.1a Local SHM digital twin on FOWT floater. 2024.

IRENA: World Energy Transitions Outlook 2023: 1.5°C Pathway. 2023.

https://doi.org/10.5194/wes-2025-110
Preprint. Discussion started: 25 August 2025

WindEurope: Floatting Offshore Wind. 2020.

Skaare, Bjørn and Nielsen, Finn and Hanson, Tor and Yttervik, Rune and Havmøller, Ole and Rekdal, Arne: Analysis of measurements and simulations from the Hywind Demo floating wind turbine: Dynamic analysis of the Hywind Demo floating wind turbine. 2014.

Skaare, Bjørn and Hanson, Tor and Nielsen, Finn and Yttervik, Rune and Hansen, Anders and Thomsen, Kenneth and Larsen, Torben and Skaare@hydro, Bjorn and No, and David, Tor and No, Finn and Gunnar, and Com, Rune and No, Anders and Melchio: Integrated dynamic analysis of floating offshore wind turbines. 2007.

Sjur Neuenkirchen Godø: Dynamic Response of Floating Wind Turbines. 2013.

Skaare, Bjørn and Nielsen, Finn and Hanson, T.D. and Yttervik, Rune and Havmøller, Ole and Rekdal, A.: Analysis of measurements and simulations from the Hywind Demo floating wind turbine. 2015.

C.P.M. Curfs: Dynamic behaviour of floating wind turbines - A comparison of open water and level ice conditions. 2015. https://repository.tudelft.nl/record/uuid:f339482a-8e0d-4827-85af-c8cf05b4260f

Cheng, Zhengshun and Wang, Kai and Gao, Zhen and Moan, Torgeir: Comparative study of spar type floating horizontal and vertical axis wind turbines subjected to constant winds. 2015.

Zhang, Lixian and Shi, Wei and Karimirad, Madjid and Michailides, Constantine and Jiang, Zhiyu: Second-order hydrodynamic effects on the response of three semisubmersible floating offshore wind turbines. 2020.

Haoran Li and Zhen Gao and Erin E. Bachynski-Polić and Yuna Zhao and Stian Fiskvik: Effect of floater flexibility on global dynamic responses of a 15-MW semi-submersible floating wind turbine. 2023.

Allen, C. and Viscelli, A. and Dagher, H. and Goupee, A. and Gaertner, E. and Abbas, N. and Hall, M.D. and Barter, G.: Definition of the UMaine VolturnUS-S Reference Platform Developed for the IEA Wind 15-Megawatt Offshore Reference Wind Turbine: IEA Wind TCP Task 37. 2020.

Loup Suja-Thauvin and Jørgen R. Krokstad and Erin E. Bachynski and Erik-Jan: Experimental results of a multimode monopile offshore wind turbine support structure subjected to steep and breaking irregular waves. 2017.

Zhixin Zhao and Wenhua Wang and Wei Shi and Shengwenjun Qi and Xin Li: Effect of floating substructure flexibility of large-volume 10 MW offshore wind turbine semi-submersible platforms on dynamic response. 2022.

Mohammed Khair Al-Solihat and Meyer Nahon: Flexible multibody dynamic modeling of a floating wind turbine. 2018.

Xiaoming Ran and Vincent Leroy and Erin E. Bachynski-Polić: Hydroelastic response of a flexible spar floating wind turbine: Numerical modelling and validation. 2023.

France Energies Marines: Contractual description – Digital Intelligent Operational Network using hYbrid SensOrs / Simulations approach. 2021.

Hirvoas, A.: Model construction of Zefyros floating offshore wind turbine. 2022.

Redoute, T.: S-MORPHO system user manual. 2020.

Gustavo Oliveira and Filipe Magalhães and Álvaro Cunha and Elsa Caetano: Continuous dynamic monitoring of an onshore wind turbine. 2018.

van Vondelen, A. A. W. and Navalkar, S. T. and Iliopoulos, A. and van der Hoek, D. C. and van Wingerden, J.-W.: Damping identification of offshore wind turbines using operational modal analysis: a review. 2022.

Masjedian, M.H. and Keshmiri, Mehdi: A review on operational modal analysis researches: Classification of methods and applications. 2009.

Miroslav Pastor and Michal Binda and Tomáš Harčarik: Modal Assurance Criterion. 2012.

https://doi.org/10.5194/wes-2025-110
Preprint. Discussion started: 25 August 2025

National Renewable Energy Laboratory (NREL): OpenFast. 2024. https://github.com/OpenFAST

Malenica, Š and Tuitman, Johan and Bigot, Fabien and Sireta, Francois-Xavier: Some aspects of 3D linear hydroelastic models of springing. 2008.

Malenica, Š and Derbanne, Quentin and Sireta, Francois-Xavier and Bigot, Fabien and Tiphine, Etienne and De Hauteclocque, Guillaume and Chen, Xiao-Bo: HOMER–Integrated hydro-structure interactions tool for naval and offshore applications. 2013.

SERCEL: SERCEL, title = S-MORPHO system – Specifications of calculation algoritms. 2024.

ANSYS: Online Manual. 2024. https://www.caee.utexas.edu/prof/kallivokas/teaching/ANSYS_examples/ansys56theory.pdf

B. J. Jonkman: TurbSim User's Guide v2.00.00 . 2016. chrome-extension://efaidnbmnnnibpcajpcglclefindmkaj/https://www.nrel.gov/wind/nwtc/assets/downloads/TurbSim/TurbSim_v2.00.pdf

Gunjit S. Bir : User's Guide to BModes (Software for Computing Rotating Beam Coupled Modes). 2007. chrome-extension://efaidnbmnnnibpcajpcglclefindmkaj/https://www.nrel.gov/wind/nwtc/assets/pdfs/bmodes.pdf

Jonkman, Jason Mark and Buhl, Marshall L and others: FAST user's guide. 2005.

Hall, Matthew: MoorDyn user's guide. 2015.

Abbas, Nikhar J and Zalkind, Daniel S and Pao, Lucy and Wright, Alan: A reference open-source controller for fixed and floating offshore wind turbines. 2022.

Hall, Matthew: Moordyn v2: New capabilities in mooring system components and load cases. 2020.

Jonkman, Jason M and Robertson, AN and Hayman, Greg J: HydroDyn user's guide and theory manual. 2014.

Molin, Bernard: Offshore structure hydrodynamics. 2023.

DNV-GL: DNV-RP-0286 Coupled analysis of floating wind turbines. 2019.

Veritas, Bureau: Classification and certification of floating offshore wind turbines. 2015.

(2013)]homb2013fatigue Homb, Hans Ranøyen: Fatigue Analysis of Mooring Lines on the Floating Wind Turbine Hywind Demo. 2013.

Johnson, Nicholas and Jonkman, Jason and Wright, A and Hayman, Greg and Robertson, A: Verification of floating offshore wind linearization functionality in OpenFAST. 2019.

Thomsen, Jonas Bjerg and Bergua, Roger and Jonkman, Jason and Robertson, Amy and Mendoza, Nicole and Brown, Cameron and Galinos, Christos and Stiesdal, Henrik: Modeling the TetraSpar Floating Offshore Wind Turbine Foundation as a Flexible Structure in OrcaFlex and OpenFAST. 2012.

Xiaoming Ran and Vincent Leroy and Erin E. Bachynski-Polić: Hydroelastic response of a flexible spar floating wind turbine: Numerical modelling and validation. 2023.

de Lauzon Jérome: Coupled eigen-frequency analysis of floating wind turbines. 2024.

Borg, Michael and Hansen, Anders Melchior and Bredmose, Henrik: Floating substructure flexibility of large-volume 10MW offshore wind turbine platforms in dynamic calculations. 2016.

Chenyu Luan and Zhen Gao and Torgeir Moan: Development and verification of a time-domain approach for determining forces and moments in structural components of floaters with an application to floating wind turbines. 2017.

Guignier, Lucie and Courbois, Adrien and Mariani, Riccardo and Choisnet, Thomas: Multibody Modelling of Floating Offshore Wind Turbine Foundation for Global Loads Analysis. 2016.

V. Leroy and E.E. Bachynski-Polić and A. Babarit and P. Ferrant and J.-C. Gilloteaux: A weak-scatterer potential flow theory-based model for the hydroelastic analysis of offshore wind turbine substructures. 2021.

https://doi.org/10.5194/wes-2025-110
Preprint. Discussion started: 25 August 2025

eawe european academy of wind energy
Open Access WIND ENERGY SCIENCE DISCUSSIONS

Kun Xu and Min Zhang and Yanlin Shao and Zhen Gao and Torgeir Moan: Effect of wave nonlinearity on fatigue damage and extreme responses of a semi-submersible floating wind turbine. 2019.